



The Society shall not be responsible for statements or opinions advanced in papers or in discussion at meetings of the Society or of its Divisions or Sections, or printed in its publications. Discussion is printed only if the paper is published in an ASME Journal. Released for general publication upon presentation. Full credit should be given to ASME, the Technical Division, and the author(s). Papers are available from ASME for nine months after the meeting.
Printed in USA.

Copyright © 1982 by ASME

On the Performance Prediction of a Centrifugal Compressor Scaled Up

T. Mashimo

Associate Professor,
Faculty of Engineering,
Meiji University,
Kawasaki, Japan
Mem. ASME

T. Sakai

Professor,
Faculty of Engineering,
Science University of Tokyo,
Tokyo, Japan

I. Ariga

Professor,
Faculty of Science
and Technology,
Keio University,
Yokohama, Japan

I. Watanabe

Professor,
Faculty of Engineering,
Kanto Gakuin University,
Yokohama, Japan
Mem. ASME

A centrifugal compressor performance prediction method, in which each loss generated within the compressor stage was estimated by recognizing the individual relationship with Mach number, was investigated over a wide range of sizes and types. Calculation formulae for the losses were established by analyzing test results. It was confirmed that the formulae could be applied to predict the performance levels of compressors with impeller diameters from 78 mm to 640 mm by referring to unpublished test data obtained experimentally by other researchers. From the results, it could be deduced that: (1) The wall friction losses and the secondary flow losses within the compressor decreased with increase of impeller size. (2) The leakage flow losses were found to increase when scaling up the compressor, even when tip clearance/blade height were held constant. The present paper presents a progress report of work still underway.

NOMENCLATURE

a	constant	z	number of blades
B	width of impeller channel, m	γ	exponent
b	height of impeller channel, m	ϵ	clearance, m
c	absolute velocity, m/s	ζ	loss coefficient
C_f	coefficient of skin friction	η	efficiency
d_m	four times hydraulic mean radius, m	η_{cal}	efficiency estimated by calculation
d_2	impeller outlet diameter, m	η_t	adiabatic temperature efficiency obtained experimentally
G	mass flow rate through a compressor stage, kg/s	κ	ratio of specific heats (= 1.4)
g	gravitational acceleration, m^2/s	ν	kinematic viscosity, m^2/s
H	loss head, m	ρ	density, kg/m^3
L	length along surface of impeller channel from inlet to outlet, m	ϕ	flow coefficient = c_{1m}/u_2
n	rotational speed, rpm		
n'	rotational speed, rps		
P	total pressure, kPa		
R	gas constant, m/K		
Re	Reynolds number		
Re_{u2}	Reynolds number = $u_2 d_2 / \nu_0$		
Re_ϵ	Reynolds number = $w_1 \epsilon / \nu$		
T	temperature, K		
u	peripheral velocity, m/s		
w	relative velocity, m/s		

SUBSCRIPTS

0	stagnation condition of impeller inlet
1	inlet condition of impeller
2	outlet condition of impeller
4	outlet condition of compressor stage
c	refer to absolute velocity
cr	refer to critical Reynolds number
df	refer to friction loss within diffuser
e	refer to expansion loss
h	refer to hub side surface
if	refer to friction loss within impeller
imp	refer to shock at inducer inlet
l	refer to leakage
m	meridional streamline direction
mix	refer to mixing loss

p refer to pressure side surface
 s refer to scroll
 sec refer to secondary flow
 sf refer to friction loss within scroll
 sh refer to shroud side surface
 su refer to suction side surface
 u tangential component

SUPERSCRIPT

— arithmetic mean from inlet to outlet of impeller

INTRDUCTION

Recently, centrifugal compressors applied to gas process plants have been exhibiting a tendency to become larger as the capacity of the plant increases. The establishment of a performance prediction method for scaled up turbomachines has been demanded, because of the difficulties of performance measurements for such turbomachines from the viewpoint of constructing the available test equipment and because of the shortage of sufficient data on the design stage.

As to the performance prediction, generally, two methods will be available. One of them is based on the hypothesis that the entire losses caused within a compressor stage would be related merely to the Reynolds number, the original form of which being expressed as follows [1-6].

$$\frac{1-\eta}{1-\eta_{ref}} = a + (1-a) \left(\frac{Re_{ref}}{Re} \right)^n \quad (1)$$

The authors investigated on the $Re-\eta$ relation like above equation before [11,12], and its results agree well with that showed in Reference [4]. The results also were referred in Reference [5], and agree well with them in the Reference. From these facts, this method of performance prediction seems to have been established completely by References [4],[5],[11],[12] and so on.

The other one of performance prediction is as follows: First, each loss generated within the compressor stage is estimated by recognizing the individual relationship between it and the velocity distribution, the Reynolds number as well as Mach number. Afterwards, the final result can be estimated by superimposing them [7-11]. Though the latter method has a troublesome defect that each loss has to be calculated one by one, it has also remarkable advantages in that the latter method can be used to predict the performance levels over the part load operating conditions of the compressor, and the latter method enable application for performance prediction of new type compressor (that is, η_{ref} in equation (1) is not yet known), while η_{ref} has to be known in case of the former. As the latter method has those advantages but has not yet been established, the purpose of the present investigation was directed mainly to establishment of each calculation formula for losses within the compressor, which would be able to apply a wide range of compressor size.

The authors have previously published prediction formulae concerning the leakage loss, secondary flow loss and so on [11,12]. When the formulae for those losses were derived, however, variations of loss levels with compressor size were not taken into account, though configurations of the impellers were taken into

consideration. Thus, in the present paper, the calculation formulae for each loss applicable regardless of the compressor sizes were surveyed by employing performance test results carried out with three compressors having impellers of 78 mm, 112 mm and 154 mm diameters respectively, in addition to the unpublished performance data for seven relatively large compressors investigated by other researchers. After applying a few corrections to some of the formulae listed in References [11] and [12], the loss formulae were found to predict the performance levels within $\pm 4\%$ in efficiency regardless of the variations of the sizes as well as the configurations, the operating conditions and the Reynolds number of the compressor.

TEST EQUIPMENT AND METHOD

Three compressors having impellers of 154, 112 and 78 mm diameters respectively were employed for the present test (hereafter, they were designated briefly as compressor A, B and C in order). Among them, compressor A (having impeller diameter of 154 mm) was the standard one, available in the market, the other two being newly constructed by the similarity configurations with respect to the standard one. The exceptions to the similarity of the configuration and dimension, however, lay in that the blade thicknesses of impellers were kept constant at 2 mm everywhere on blades for the three compressors, and that the cross sectional areas of the scrolls were constructed in no proportion to the impeller diameter. Outlines of those compressors are shown in Fig.1, and the specifications of the compressor A are listed in Table 1.

A closed circuit ducting system was employed for the present test (Fig.2). The Reynolds number was varied by altering air pressure in an air chamber located upstream of the compressor. Air pressure in the chamber was varied from 30 to 100 kPa by means of a vacuum pump. Air temperature in the air chamber was kept constant at 313 ± 1 K by using a heat exchanger, and the temperature was monitored by means of a mercury thermometer having 0.1 K scale.

The air flow to the compressor was made adjustable by means of a flow regulatory valve located upstream in the air chamber and was measured by a nozzle situated upstream of the compressor.

The compressor rotational speed was adjusted by varying the flow rates of compressed air (delivered by means of a Roots blower) to a radial inflow turbine driving the compressor. The speed was monitored by means of a digital counter.

The total pressure and the total temperature at the compressor stage outlet were measured at the center of diameter of a delivery pipe by means of a Kiel probe and a copper-constantan thermocouple, respectively.

Table 1 Specifications of compressor A

Impeller outlet diameter	154 mm
Outer diameter at impeller inlet	86 mm
Inner diameter at impeller inlet	32 mm
Impeller outlet blade height	8 mm
Impeller outlet blade thickness	2 mm
Clearance height	0.4 mm
Number of blades	14
Maximum rotational speed	41000 rpm
Pressure ratio	2
Delivery volume flow rate	30 m ³ /min

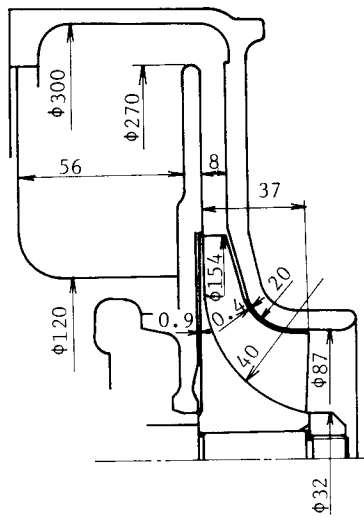


Fig. 1(a) Compressor A

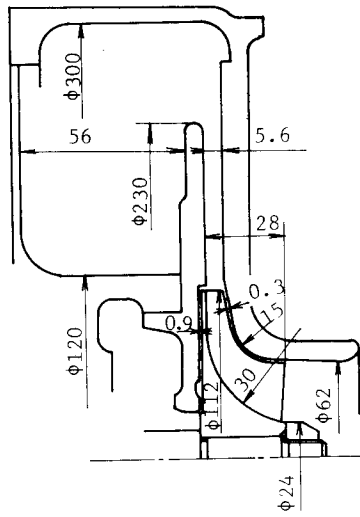


Fig. 1(b) Compressor B

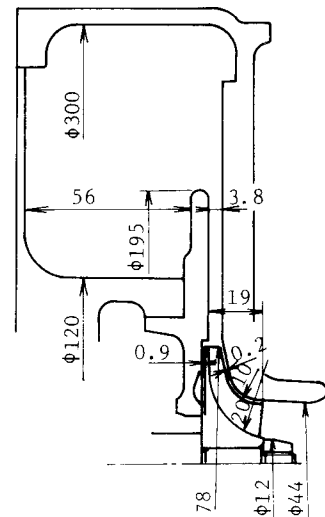
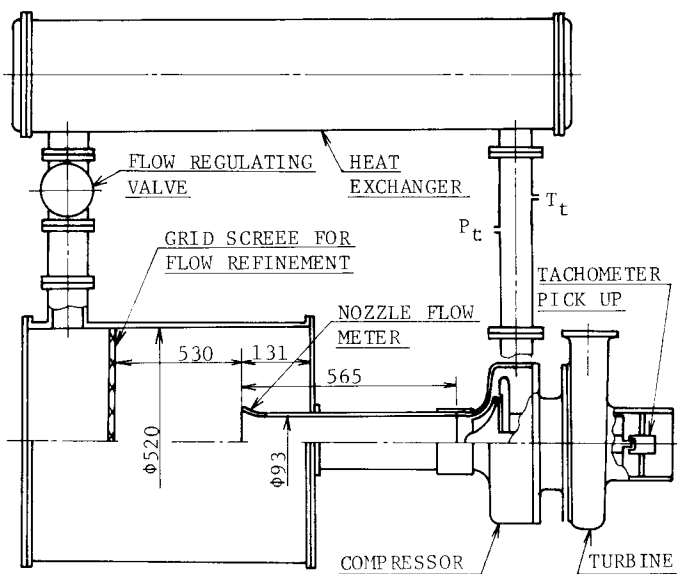


Fig. 1(c) Compressor C



P_t : Location of Total Pressure Probe

T_t : Location of Total Temperature Probe

Fig. 2 Schematic drawing of the compressor test equipment

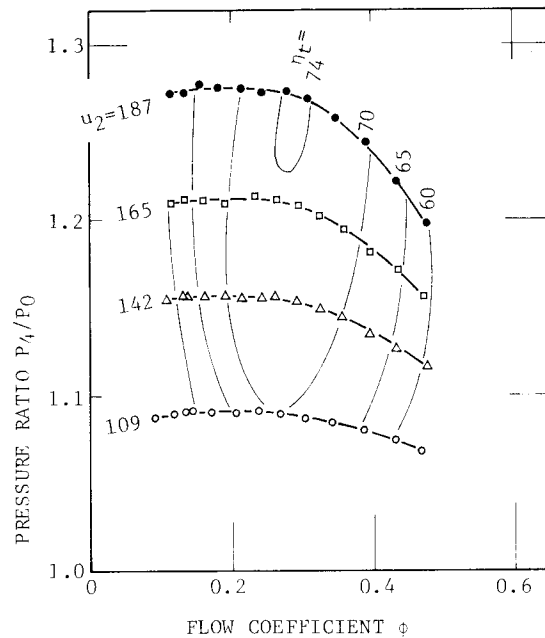


Fig. 3(a) Performance curves of compressor A

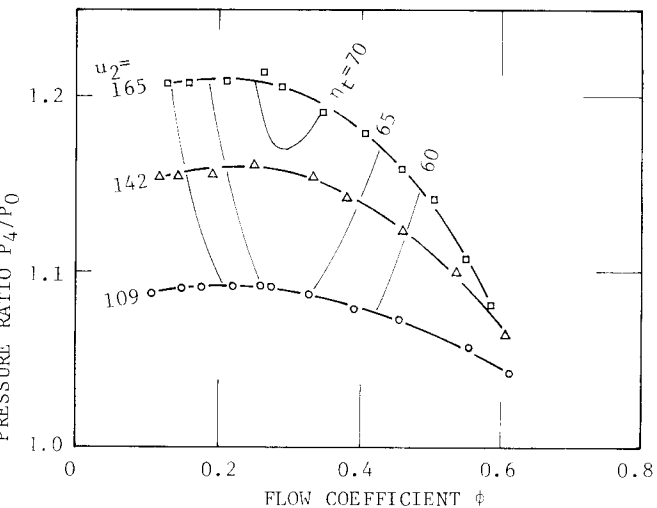


Fig. 3(b) Performance curves of compressor B

EXPERIMENTAL RESULTS

The pressure ratios and the adiabatic temperature efficiencies for compressor A, B and C are plotted versus flow coefficients, the peripheral speeds being adopted parameters, as shown in Fig.3, when the pressure in the air chamber was kept at atmospheric. The adiabatic temperature efficiencies in the figures were evaluated by using the following expression.

$$\eta_t = \frac{T_0 [(P_4/P_0)^{\frac{\kappa-1}{\kappa}} - 1]}{T_4 - T_0} \quad (2)$$

Fig.4 shows an example of the variations of the pressure ratios as the size of the compressor becomes larger at a speed of $u_2=142$. At other speeds measured, the variations revealed the similar tendency to that in Fig.4, showing that the effect of compressor size on pressure ratio was very small.

On the other hand, variations of the efficiency as the size of the compressor becomes larger are shown in Fig.5. In this diagram, it is seen that the peak efficiency of compressor A was 73 % while the efficiency of compressor C was at most about 63 %. In addition, the efficiency differences become higher for the smaller flow coefficients as the size of the compressor is increased.

The efficiency increase with the scaling up of the compressor size can be attributed mainly to the dimensional differences among the compressors. These dimensional differences are quantified by not only the Reynolds number Re_{u2} but also tip clearance ϵ of the

impeller (The relation among ϵ , Re_{u2} and η could be estimated with the results published by the authors before [11], and the relation among them was not treated in this investigation)

Confirmation of the validity of this argument is illustrated in Fig.6, which shows an example of relationship between the efficiency and the Reynolds number under the same peripheral velocity and the same flow coefficient. Though the plotted points are distributed within a comparatively broad band especially in the low Reynolds number region, differences in efficiencies among the different compressors become smaller than that at $\phi=0.17$ in Fig.5. Hence, it could be safely said that the larger part of the performance gap among the various compressor sizes examined would be due to the differences of the Reynolds number of the compressor and the tip clearances.

DISCUSSION

Variations of the loss levels generated within compressor stages as the compressor sizes became larger were surveyed. As the compressors employed for the present test were of relatively small sizes, the experimental data (unpublished) obtained by other researchers using compressors having comparatively large sizes were added to the present experimental data for the subsequent analysis in order to enable prediction of the performance of the larger compressor sizes.

The outlines of the compressors referred to the analysis of the loss levels, in other words, to the estimation of the performances, were illustrated in Fig.7

First, velocity distributions within the impellers were obtained by using methods by Hamrick [13] and

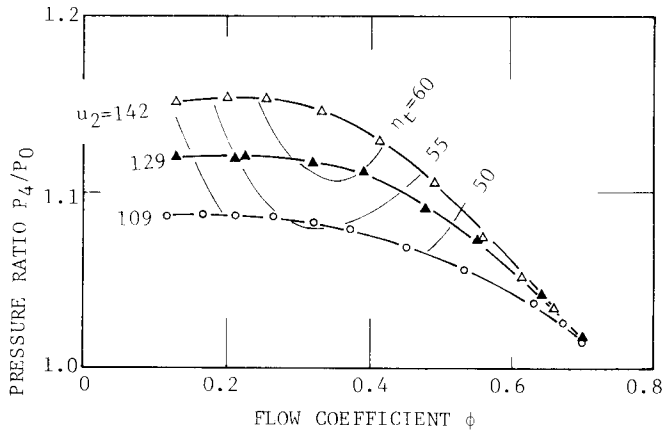


Fig.3(c) Performance curves of compressor C

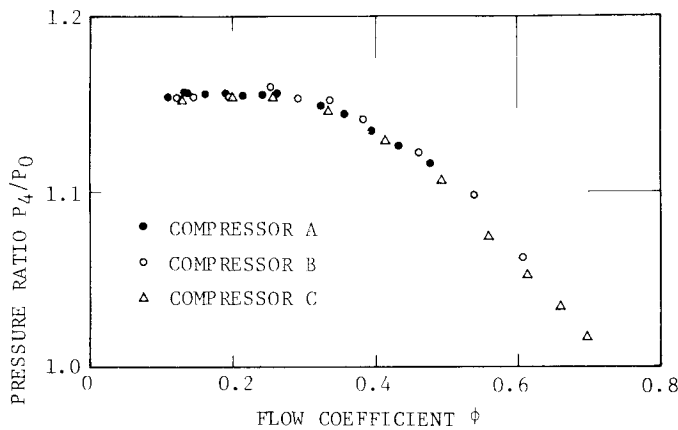


Fig.4 Relation between flow coefficient and pressure ratio ($u_2=142$)

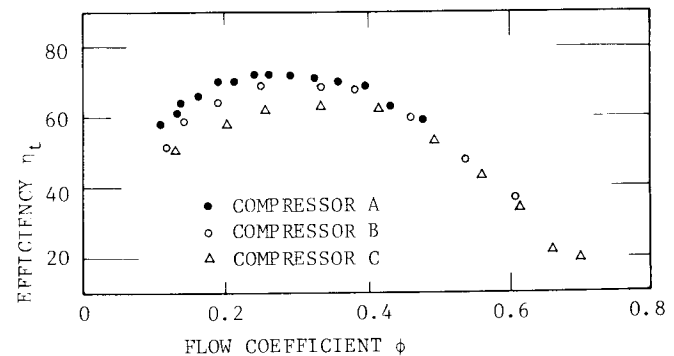


Fig.5 Relation between flow coefficient and efficiency ($u_2=142$)

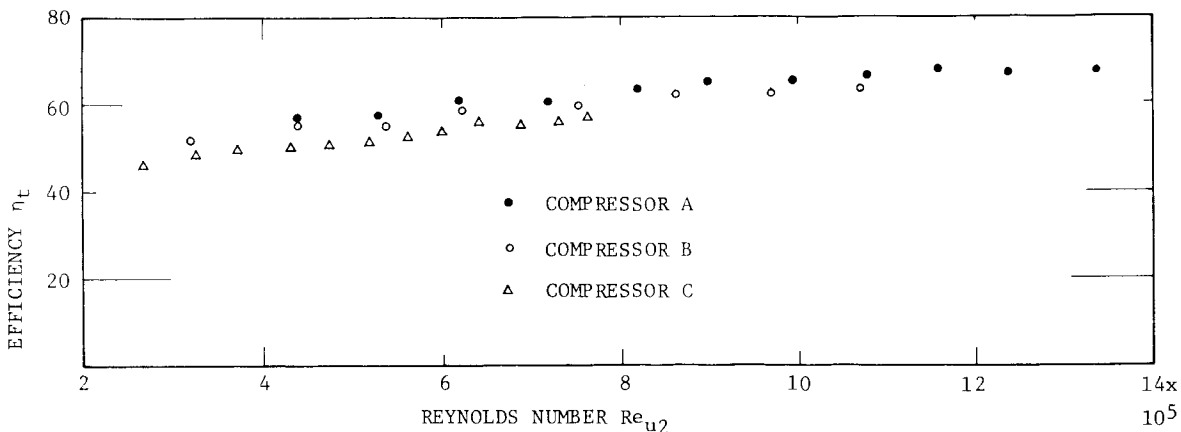


Fig.6 Relation between Reynolds number and efficiency ($\phi = 0.17$, $u_2=142$)

others [12]. The loss levels were calculated by substituting corresponding velocities obtained above into the following equations (refer corresponding literature numbered as to details of the following equations).

(a) Shock loss at an inducer inlet H_{imp} [11][12],

$$H_{imp} = c_{imp}^2 / (2g) \quad (3)$$





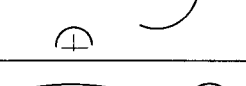

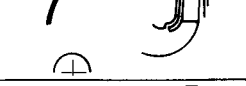



DESIGNATION	d_2 (mm)	b_2 (mm)	z	u_2	CONFIGURATION OF COMPRESSOR
A	154	8	14	150 100	
B	112	5.6	14	150 100	
C	78	3.8	14	150 100	
D	420	31	20	315 285	
E	420	23	22	300 240	
F	640	16	14	323 294	
G	640	16	16	323 294	
H	280	16	14	337	
I	250	15	18	328	
J	207	9.2	16	365	

Fig. 7 Outlines of compressors employed for performance Prediction

(b) Wall friction loss within impeller channels H_{if} [11],

$H_{if} = H_p + H_{su} + H_{sh,w} + H_h$ (for impellers of compressors D, E, F and G in Fig.7, that is, for double shrouded impellers) (4-1)

$H_{if} = H_p + H_{su} + H_{sh,c} + H_h$ (for impellers of compressors A, B, C, H, I and J, that is, for single shrouded impellers) (4-2) where,

$$H_p = \frac{\overline{w_p^2} L_p \overline{b}}{2g \overline{b} \overline{B}} C_{fp}, \quad C_{fp} = 0.074 / \left(\frac{\overline{w_p^{0.2}} L_p^{0.2}}{v_p^{0.2}} \right)$$

$$H_{su} = \frac{\overline{w_{su}^2} L_{su} \overline{b}}{2g \overline{b} \overline{B}} C_{fsu}, \quad C_{fsu} = 0.074 / \left(\frac{\overline{w_{su}^{0.2}} L_{su}^{0.2}}{v_{su}^{0.2}} \right)$$

$$H_{sh,w} = \frac{\overline{w_{sh}^2} L_{sh,w} \overline{B}}{2g \overline{b} \overline{B}} C_{fsh,w},$$

$$C_{fsh,w} = 0.074 / \left(\frac{\overline{w_{sh}^{0.2}} L_{sh,w}^{0.2}}{v_{sh}^{0.2}} \right)$$

$$H_{sh,c} = \frac{\overline{c_{sh}^2} L_{sh,c} \overline{B}}{2g \overline{b} \overline{B}} C_{fsh,c},$$

$$C_{fsh,c} = 0.074 / \left(\frac{\overline{c_{sh}^{0.2}} L_{sh,c}^{0.2}}{v_{sh}^{0.2}} \right)$$

$$H_h = \frac{\overline{w_h^2} L_h \overline{B}}{2g \overline{b} \overline{B}} C_{fh}, \quad C_{fh} = 0.074 / \left(\frac{\overline{w_h^{0.2}} L_h^{0.2}}{v_h^{0.2}} \right)$$

(c) Wall friction loss within a diffuser H_{df} [11][15],

$$H_{df} = \zeta_{df} \frac{c_2^2}{2g} \quad (5)$$

(d) Wall friction loss within a scroll H_{sf} [11][16],

$$H_{sf} = \zeta_{sf} \frac{c_s^2}{2g} \quad (6)$$

(e) Sudden expansion loss at a scroll inlet H_e [11][17],

$$H_e = \frac{(c_{3,u} - c_s)^2 - c_{3,m}^2}{2g} \quad (7)$$

(f) Leakage loss between neighbouring impeller channels H_l [12],

$$H_l = \frac{0.375 (g \kappa R T_0)^{0.5}}{u_2} \left[0.013 \left(\frac{\epsilon}{d_m} Re_{u2} Re_\epsilon \right)^{0.13} \right. \\ \left. \times \frac{0.04}{(u_2 / \sqrt{g \kappa R T_0})} \left(\frac{G_i - G_b}{G_c} \right)^{0.2} \frac{u_2^2}{g} \right] \quad (8)$$

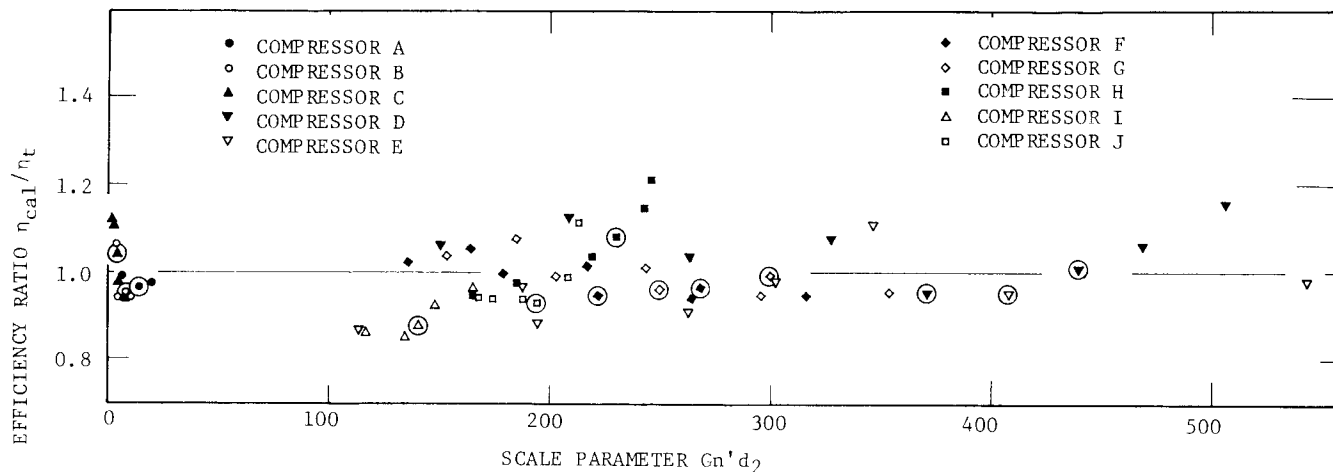


Fig.8 Relation between scale parameter and efficiency

(g) Secondary flow loss within impeller channels H_{sec} [11],

$$H_{sec} = c_{sec} \left[\frac{\sin \beta_2}{(2w_2/u_2) - [\cos \beta_2 + (r_2/R_b)(w_2^2/u_2^2)]} \right]^{0.3} \times \frac{w_2^2}{2g} \frac{L}{d_m} \quad (9)$$

(h) Mixing loss at a impeller outlet H_{mix} [11][15]

$$H_{mix} = \frac{1}{1+\lambda^2} \left[\frac{(\delta_b + \delta_w)/(2\pi r_2/z)}{1 - (\delta_b + \delta_w)/(2\pi r_2/z)} \right]^2 \times \frac{c_2^2}{2g} \quad (10)$$

The stage efficiencies based on the above losses η_{cal} were evaluated by using the following formula,

$$\eta_{cal} = 1 - \frac{H_{imp} + H_{if} + H_{df} + H_{sf} + H_e + H_i + H_{sec} + H_{mix}}{u_2 c_{2u}/g} \quad (11)$$

Fig.8 shows ratios of the efficiencies η_{cal} obtained by the above-mentioned calculation to η_t obtained experimentally for the compressors illustrated in Fig.7.

The measure of largeness of the compressor is not only size of impeller diameter, but also size of blade height as well as magnitude of rotation speed of the impeller. On the other hand, flow rate G through the compressor is related to the impeller diameter d_2 and the blade height b_2 in addition to the rotation speed n' . Therefore, it is conceivable that the largeness could be related mainly to the impeller diameter d_2 , rotation speed n' and flow rate G in place of the blade height b_2 . The purpose of the present investigation is to try to improve accuracy of the present performance prediction method when compressor is scaled up, that is, when d_2 , n' and G are increased independently. If the Reynolds number Re_{u_2} used commonly is adopted as the abscissa of Fig.8, the accuracy of the performance prediction with increasing flow rate G can not be shown in the figure, though that with increasing of d_2 and n' can. From those point of view, a non-dimensional parameter $Gn'd_2/\rho_0 v_0^2$ was tentatively considered as a measure of largeness of the compressor [19]. In Fig.8, however, parameter $Gn'd_2$ was adopted as the abscissa, which was simplified by neglecting the product $\rho_0 v_0^2$ in the non-dimensional parameter, because it remained a common factor over the whole test data referred to.

Though compressors F and G were installed with the return-channel without scroll, calculations of the loss levels for them were carried assuming they were installed with a suitable scroll, because the appropriate prediction formula for loss levels caused within the actual return channel was unavailable.

Compressors H and I were them with vaned diffuser. Loss levels for H_{df} of those compressors, however, were calculated by using equation (5) derived for vaneless diffuser because of a lack of appropriate calculation formula for loss within the vaned diffuser.

The points in Fig.8 show wider scattering than those obtained from equation (1), for the performance prediction method employed to calculate the data in Fig.8 is a method which is still being developed as mentioned above, while the method by equation (1) has been completely established. Refinement of the present method by future authors is expected to improve its accuracy by better definition of the component terms. The points in the figure seem to distribute around a line $\eta_{cal}/\eta_t = 1$ within $\pm 4\%$ in efficiency, in spite of the variations of the operating conditions and the configurations of the elements constructing the compressor as well as the largeness of the compressors. The marks enclosed within the circles in the figure correspond to the operating conditions for the design point or for the no shock inflow at the inducer inlet of the respective compressors.

The compressor Reynolds number Re_{u_2} of some of the compressors listed in Fig.7 were above 10^7 . It has been frequently reported in the open literature that the critical Reynolds number dividing the two regions, in which the compressor efficiencies were affected by either the Reynolds number or the surface roughness, would be the order of 10^6 [4]. When the critical Reynolds number of 10^6 is assumed, one might be apprehensive that the term of the critical Reynolds number has not been taken into account on the performance estimations afore-mentioned, in spite of the fact that the Reynolds numbers Re_{u_2} of some compressors amount to above 10^7 . The reasons why the critical Reynolds number has not been taken into account, are as follows: First, relationship between each loss within the compressor and the critical Reynolds number for the loss are not yet clarified. Second, when the critical Reynolds number is assumed to be $Re_{u_2,cr} = 10^6$, difference between friction factors at $Re_{u_2} = 10^6$ and $Re_{u_2} = 10^7$ is analogized to be small (about 1% of losses depending on the Reynolds number) from resistance formula for rough circular pipe [18], so far as Re_{u_2} is varied by altering merely the impeller diameter while the

rotation speed of the impeller, viscosity of the fluid as well as the surface roughness are unaltered.

Based on the success for the prediction of the efficiency within $\pm 4\%$, variations of levels of losses aforementioned [equations from (3) to (10)] as compressor A was scaled up under the completely similar configuration were surveyed theoretically by applying the calculation formulae for the losses. Compressor A was selected as the prototype, and the impeller diameter was scaled up from 154 mm (of the prototype) to 750 mm.

Fig.9 shows the efficiency thus estimated. The flow coefficient was adopted as abscissa, the parameter being the diameters of the impellers. From the figure, it could be seen that the larger the impeller diameter, the higher the efficiency. In addition, the peak efficiency corresponding to each impeller diameter has a tendency to shift to the region having larger flow coefficients as the impeller diameter increases so far as the same peripheral velocity u_2 is maintained. It is recognized, furthermore, that the rate of increment in the compressor efficiency $\Delta\eta/\Delta d_2$ becomes smaller in proportion to the impeller diameter.

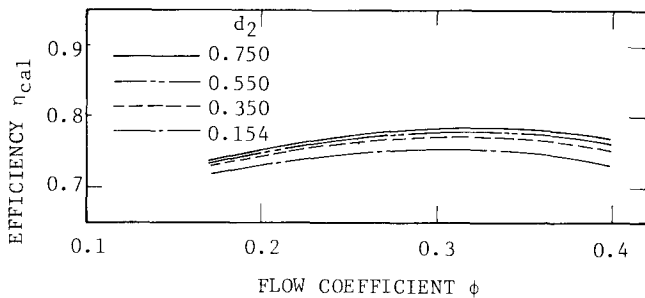


Fig. 9 Variation of Relation between flow coefficient and efficiency

Such tendency of the rate of increment in the compressor efficiency is exhibited concretely in Fig.10. The figure shows that the larger the flow coefficients, the larger the increments of the efficiencies as the compressor is scaled up.

In Fig.11, levels of various losses caused within the compressor stage are shown as the ratios of the losses to the theoretical head $u_2 c_{2u}/g$. In the figure, the friction loss within the diffuser H_{df} shows the largest level over the whole range of the flow coefficients, and this loss has a tendency to increase with decreasing flow coefficient. The expansion loss at the diffuser outlet H_e and the secondary flow loss within the impeller H_{sec} exhibited larger levels, and the loss H_e has the same tendency with the loss H_{df} , while the loss H_{sec} increases as the flow coefficient increases.

On the other hand, variations of loss levels by the scaling up of the compressor sizes are illustrated in Fig.12. The abscissa is the impeller diameter, and the ordinate denotes the loss rate. From the figure, the following results are deduced. Under the condition of the same flow coefficients, the wall friction loss within the impeller channel H_{if} and that within the diffuser H_{df} decreases to some extent with increasing impeller sizes. The secondary flow loss within the impeller channel H_{sec} exhibits also the same trend as H_{if} , the rate of decrease, however, being larger than that of H_{if} . The leakage loss occurring between the neighbouring impeller channel H_l increases with enlargement of the impeller size, contrary to the case of H_{if} . As to H_{imp} , H_e and H_{mix} , it is seen from Fig.12 that those losses are invariant even when the impeller diameter is increased.

Finally, calculations were performed to find out what variations of the performance efficiency would occur, when some improvements would be applied to the compressor in addition to the scaling up. Fig.13 shows examples of the results. In the figure, curve (1) denotes that the efficiency increase amounts to 4% de-

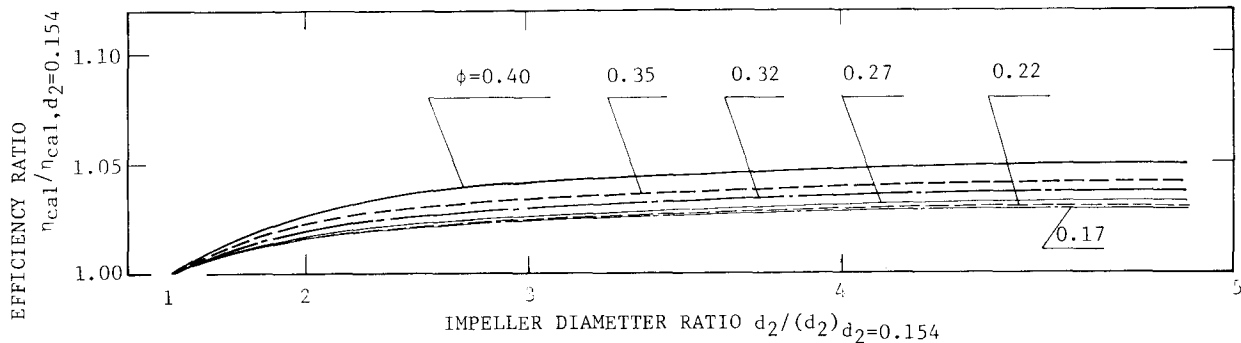


Fig.10 Variation of relation between impeller diameter ratio and efficiency ratio ($u_2=300$)

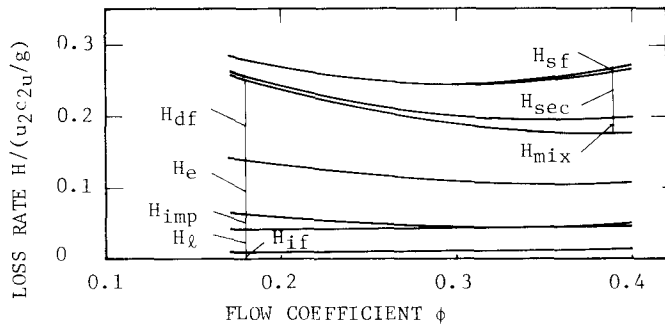


Fig.11(a) Relation between flow coefficient and loss rate for compressor A ($d_2=0.154$, $u_2=300$)

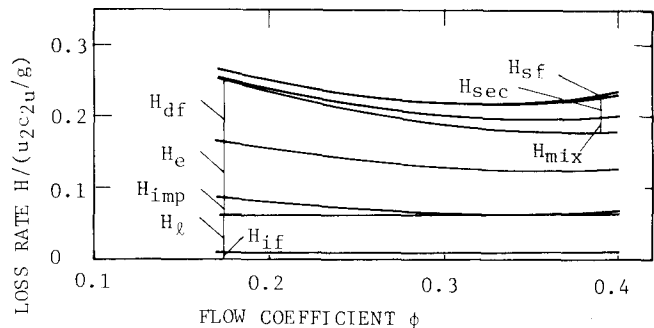


Fig.11(b) Relation between flow coefficient and loss rate ($d_2=0.750$, $u_2=300$)

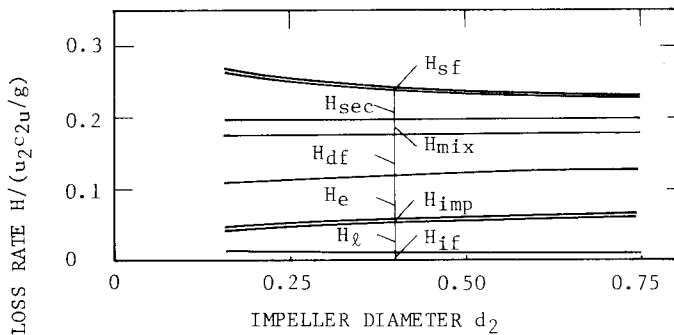


Fig.12(a) Variation of loss rate with impeller diameter ($\phi = 0.4$)

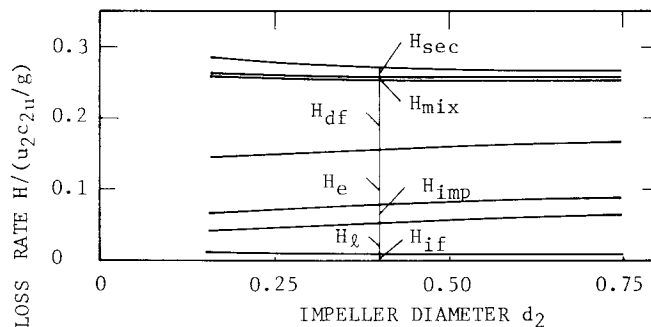


Fig.12(b) Variations of loss rate with impeller diameter ($\phi = 0.17$)

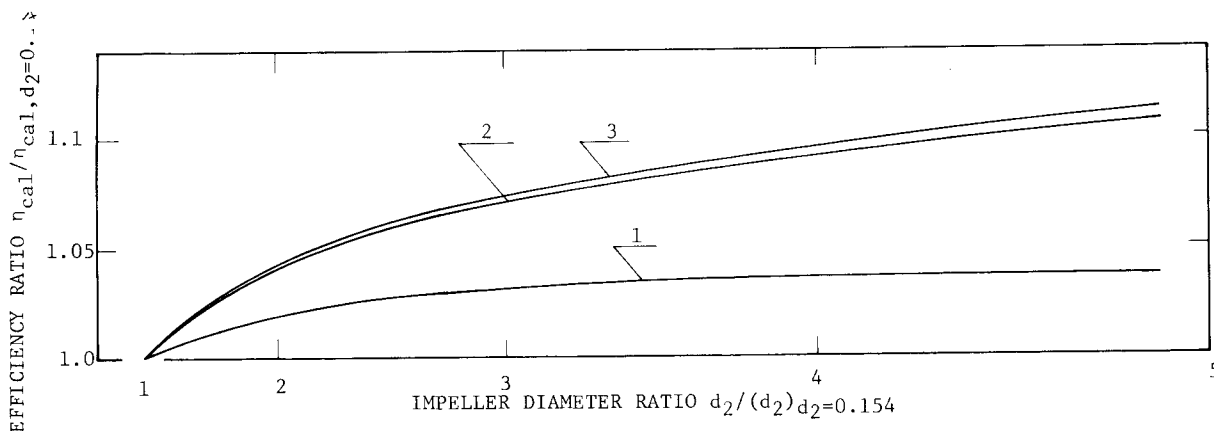


Fig.13 Efficiency increment with scale up and remodel ($u_2=300$)

pending on the effects of Re , tip clearance and so on when the impeller diameter is increased, for instance, from 154 mm to 750 mm under completely similar conditions of the compressor. On the other hand, curve (2) denotes efficiency increase in the particular case when the tip clearance only is held constant at that of compressor A (having the smallest impeller of $d_2=154$ mm) though the compressor is scaled up. That is, curve (2) shows rather the possibility that the compressor efficiency could be elevated up to curve (2) by holding constant tip clearance in spite of the scale up of the compressor. Curve (3) shows the possibility of the efficiency increase on the compressor remodeled by decreasing the blade thickness up to it corresponding to compressor A in addition to the scale up and the improvement on the tip clearance.

CONCLUSIONS

1 Loss prediction formulae were derived, and it was found that the formulae could be applied under error within $\pm 4\%$ to the compressor having impeller diameter from 154 mm to 640 mm regardless of the differences of the configurations of the elements composing the compressor as well as the operating conditions.

2 The efficiency increment amounted to 10% under the combined improvement effects both due to the scale up and the reduction of the tip clearance, while the efficiency increment by 4% being attained by means of the mere scaling up of the impeller diameter from 154 mm to 750 mm.

3 It was found that the larger the flow coefficient, the larger the increment in the efficiency of compressor scaled up.

4 The wall friction losses within the impeller channels and the diffuser decreased to some extent with increasing impeller diameters. The secondary flow losses within the impeller channels exhibited also the same trend with above, the decreasing rate being enlarged.

5 The leakage loss level was found to increase by the scaling up of the compressor, even when tip clearance/blade height were held constant.

ACKNOWLEDGEMENTS

The project of the present experimental study was conducted as a work of Subdivision Committee Concerning Performances of Large Scaled Turbomachines, which belongs to the Joint Committee of the Japan Society of Mechanical Engineers, and it was sponsored by the following companies (in alphabetical order): Dengyosha Machine Works, Ehara Mfg. Co., Fuji Electric Co., Hitachi, Hitachi Shipbuilding and Engineering Co., Ishikawajima-Harima Heavy Industries, Kawasaki Heavy Industries, Kobe Steel, Mitsubishi Electric Corp., Mitsui Shipbuilding and Engineering Co., Nagasaki Shipyards and Engine Works of Mitsubishi Heavy Industries, Nippon Kokan, Sumitomo Heavy Industries, Takasago Technical Institute of Mitsubishi Heavy Industries, Unozawa-Gumi Iron Works.

The authors wish to express their heartfelt thanks for the permission of this presentation as well as their sponsorship. In addition, the experimental study was very much helped by Takeshi Miyashita, and Masao Nakamura, of Ishikawajima-Harima Heavy Industries, Hideaki Baba, Kaoru Tanigawa, Students of Meiji University, to whom the authors wish to express their

sincere thanks.

REFERENCES

- 1 Ippen, A. T., "The Influence of Viscosity on Centrifugal-Pump Performance," Trans. ASME, Vol. 68, No. 8, Nov. 1946, pp. 823.
- 2 Davis, H., Kottas, H., and Moody, A. M. G., "The Influence of Reynolds Number on the Performance of Turbomachinery," Trans. ASME, Vol. 73, No. 5, July 1951, pp. 499.
- Warner, J., and Misoda, J., "Correlation of Reynolds Number Effect for a Family of Small Centrifugal Compressors," ASME Paper No. 63-AHGT-97, March 1963.
- 4 Heidelberg, L. J., Ball, C. L., and Weigel, C., "Effect of Reynolds Number on Overall Performance of a 6-inch Radial Blade Centrifugal Compressor," NASA TN D-5761, April 1970.
- 5 Wiesner, F. J., "A New Appraisal of Reynolds Number Effects on Centrifugal Compressor Performance," ASME Journal of Engineering for Power, Vol. 101, No. 3, July 1979, pp. 384.
- 6 Mashimo, T., Watanabe, I., and et al., "Effect of Reynolds number on Performance Characteristics of a Centrifugal Compressor," ASME Paper No. 71-GT-25, March 1971.
- 7 Bullock, R. O., "Analysis of Reynolds Number and Scale Effects on Performance of Turbomachinery," ASME Journal of Engineering for Power, Vol. 86, No. 3, July 1964, pp. 247.
- 8 Balje, O. E., "A Study on Reynolds Number Effects in Turbomachines," ASME Journal of Engineering for Power, Vol. 86, No. 3, July 1964, pp. 275.
- 9 Senoo, Y., "Performance of Centrifugal Compressor and Reynolds Number," Journal of the Japan Society of the Mechanical Engineers, Vol. 70, No. 579, April 1967, pp. 583.
- 10 Galvas, M. R., "Fortran Program for Predicting Off-Design Performance of Centrifugal Compressor," NASA TN D 7487, 1972.
- 11 Mashimo, T., Watanabe, I., and et al., "Effects of Reynolds Number on Performance Characteristics of a Centrifugal Compressor, With Special Reference to Configurations of Impellers," ASME Journal of Engineering for Power, Vol. 97, No. 3, July 1975, pp. 361.
- 12 Mashimo, T., Watanabe, I., and et al., "Effects of Fluid Leakage on Performance of a Centrifugal Compressor," ASME Journal of Engineering for Power, Vol. 101, No. 3, July 1979, pp. 337.
- 13 Hamrick, J. H., and et al., "Method of Analysis for Compressible Flow through Mixed-Flow Centrifugal Impellers of Arbitrary Design," NACA TN 2165, 1950.
- 14 Ferguson, T. B., "The Centrifugal Compressor Stage," Butterworths, London, 1963, pp. 53.
- 15 Johnston, J. P., and Dean, R. C., "Losses in Vaneless Diffusers of Centrifugal Compressors and Pumps," ASME Journal of Engineering for Power, Vol. 88, No. 1, Jan. 1966, pp. 49.
- 16 Ito, H., "Friction Factor for Turbulent Flow in Curved Pipes," ASME Journal of Basic Engineering, Vol. 81, No. 2, Jun 1959, pp. 123.
- 17 Shirakura, M., "Effect of Surface Roughness in Impeller Channel on Performance of Volute Pump," Journal of the Japan Society of the Mechanical Engineers, Vol. 62, No. 485, Jun 1959, pp. 890.
- 18 Schlichting, E., "Boundary-Layer Theory," McGRAW-HILL, New York, 1968, pp. 583-589.
- 19 Watanabe, I., "The Dimensional Analysis," Gihodo, Tokyo, 1961, pp. 106.